Fifth International Symposium on Marine Propulsors
smp'17, Espoo, Finland, June 2017

Modified BEM Methods for the Marine Current Turbine Performance Analysis under Non-uniform Inflow Condition

Hang Li [1,2,3], Long Yu[1,2,3], Yanping He[1,2,3]

[1] State Key Laboratory of Ocean Engineering, Shanghai Jiao Tong University(SJTU), Shanghai 200240, China

[2] Collaborative Innovation Center for Advanced Ship and Deep-Sea Exploration(CISSE), Shanghai 200240, P.R. China

[3] School of Naval Architecture, Ocean & Civil Engineering, Shanghai Jiaotong University(SJTU), Shanghai 200240, China

ABSTRACT

Marine Current Turbines(MCTs) are crucial devices for marine renewable energy exploration, while numerical calculation of their performance is a significant aspect of research in this territory. Computational Fluid Dynamics(CFD) and Blade Element Momentum Theory(BEMT) are effective tools for performance prediction of MCTs. In this paper, two modified BEMT approaches, Transient-Integration(TI-BEMT) and Time-Averaged(TA-BEMT), are developed for MCT performance simulation non-uniform inflow, which conventional theory is inapplicable for, and results of them are validated by comparison with CFD. CFD simulation is carried out with both analysis options of steady state and transient, to investigate impact of transient behavior on non-uniform flow field. The work demonstrates that the numerical model developed in this paper is a functional and efficient tool for performance prediction for MCTs that work in non-uniform inflow, and TI-BEMT is more recommendable between the two BEMT approaches.

Keywords

MCTs; BEMT; non-uniform inflow; transient analysis; CFD simulation.

1 INTRODUCTION

Research of marine current exploration devices has been a promising field in renewable energy industry in recent years, and Marine Current Turbines (MCTs) have always been crucial equipment in ocean energy exploration. Computational Fluid Dynamics (CFD) and Blade Element Momentum Theory (BEMT) are two effective tools for analysis for the performance.

BEMT is a numerical method based on discretization. A blade is discretized radially as several blade elements and thrust and torque acting on each blade element is solved individually, thus the total thrust and torque acting on the blade is solved by numerical integration. Given the feature of simple but efficient, BEMT has become an effective tool in marine current exploration industry, for both performance prediction and optimum design of blades(Yu, L., et al.(2016)).

Conventional BEMT is developed based on steady uniform inflow(Wang, Y. et al(2014)). In fact, due to the existence of viscous friction of the sea bed, inflow velocity has a non-uniform profile in vertical direction, which has significant effect on performance of turbines. The local inflow velocity of each blade element varies when rotating, therefore conventional theory can not be applied directly. Despite CFD is an effective tool for performance analysis in non-uniform inflow, it is necessary to developed a more efficient approach, and modified BEMT(M-BEMT) is a promising option.

CFD is an effective approach for performance simulation in non-uniform, which is adaptive for complex inflow condition, and provides detailed information of the flow field. Klein, L. et al (2016) investigated performance of wind turbines in jet flow, while performance of MCTs in non-uniform inflow can be solved by this approach as well.

In this paper, two modified approaches are developed based on non-uniform inflow. One of them is known as Transient Integration approach(TI-BEMT), which solves transient loads acting on blades by modifying the equations in conventional theory. Averaged thrust and torque are solved by integrating transient loads in a period of rotation.

The other approach eliminates non-uniformity of inflow by time-averaging, known as Time-Averaged approach(TA-BEMT), which functions as a simplification of equations developed in the first approach. This approach is more efficient than the first one, but not applicable for unsteady inflow or highly non-uniform inflow.

Both approaches are applied for performance prediction of a three-bladed turbine in shear flow, and validated by comparing results with CFD. For CFD simulation, both transient and steady analyses are carried out, to quantify the impact of transient behavior on this flow field. Results denote that both M-BEMT approaches have sufficient precision.

2 THEORETICAL BACKGROUND OF BEMT

2.1 Conventional theory of BEMT

Procedure of applying BEMT for performance prediction for MCTs is given by Figure 1.

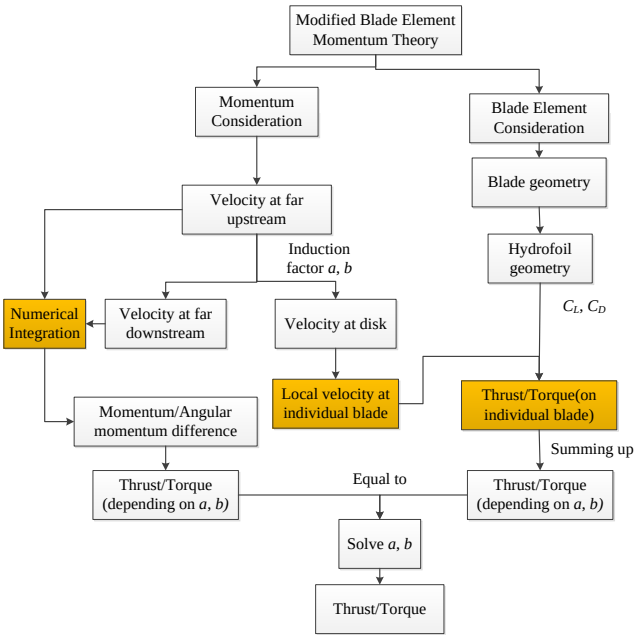

Figure 1 Procedure of BEMT application for MCTs

BEMT consists of two parts, momentum consideration and blade element consideration. In momentum consideration, thrust and torque acting on an annulus area on the blade disk equal to the difference of momentum and angular momentum. For an annulus area with radius r and width Δr, thrust and torque can be expressed by Eqs. (1) and (2).

$$\Delta T = 4\pi r \Delta r \rho U_1^2 a(1-a) \tag{1}$$

$$\Delta Q = 4\pi r^3 \Delta r \rho U_1 \Omega (1-a) b \tag{2}$$

where U_1 is velocity of inflow, and axial factor a and tangential induction factor b are unknown parameters need to be solved. The relations are shown in Figure 2.

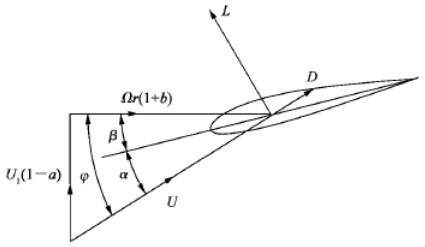

Figure 2 Velocity triangle

In blade element consideration, lift and drag forces acting on a blade element are calculated based on hydrodynamic coefficients of 2D foil section. Thrust and torque acting on all blade elements with radius r combined can be expressed by Eqs. (3) and (4):

$$\Delta T = \tfrac{1}{2}\rho N (C_L \cos\varphi + C_D \sin\varphi) \cdot U_1^2 c \Delta r (1-a)^2 / \sin^2\varphi \tag{3}$$

$$\Delta Q = \tfrac{1}{2}\rho N (C_L \sin\varphi - C_D \cos\varphi) U_1^2 c \Delta r (1-a)^2 / \sin^2\varphi \tag{4}$$

where c is local chord length, N is number of blades, and φ is attack angle of inflow at the blade element, which is related to a and b, and equations for them can be yielded to Eqs(5),(6) by combining Eqs. (1)~(4).

$$a = \frac{cN(C_L \cos\varphi + C_D \sin\varphi)}{cN(C_L \cos\varphi + C_D \sin\varphi) + 8\pi r \sin^2\varphi} \tag{5}$$

$$b = \frac{cN(C_L \sin\varphi - C_D \cos\varphi)}{8\pi r \sin\varphi\cos\varphi - cN(C_L \sin\varphi - C_D \cos\varphi)} \tag{6}$$

Eqs. (5) and (6) can be solved by iteration, which is the essence of BEMT. They link forces and induction factors together. Thrusts and torques on blade elements can be solved by Eqs.(3) and (4). Once induction factors are solved, and total loads on the whole blades can be solved by numerical integration.

2.1 Modification required of application of BEMT in non-uniform inflow

Three steps in Figure 1 are highlighted, which have more complicity when inflow is non-uniform. Firstly, in momentum consideration of conventional BEMT, momentum and angular momentum on an annulus area at the radius can be calculated by multiplying velocity with the area, since the inflow is uniform. While for non-uniform inflow, momentum and annular momentum have to be solved by integrating velocity on the annulus area. Therefore, equations in momentum consideration have to be modified.

Secondly, in blade element theory, forces acting on a blade element are calculated based on local velocity, which can be obtained by multiplying inflow velocity and induction factor. In conventional theory, forces are independent of circumferential location, because the inflow velocity is uniform and local velocity doesn't vary with the rotation. However, local velocity on a blade element varies with rotation when inflow velocity is non-uniform, so thrust and torque acting on blade elements depend on circumferential location.

Thirdly, since the local velocity at each blade element is not equal in non-uniform inflow, forces acting on all *N* blade elements cannot be presumed to be equal. Instead, they have to be calculated individually, and total force has to be solved by summing them up.

In summary, for MCTs in non-uniform inflow, conventional BEMT has to be modified to adjust the features of inflow.

3 MODIFICATION OF BEMT FOR NON-UNIFORM INFLOW

3.1 Transient application of conventional BEMT

Previous research has provided an approach to solve transient loads on turbines in shear inflow(Batten, W.M.J. et al. (2008)). An *N*-bladed turbine is simplified to be summation of *N* single blade, and for each blade at specific circumferential location, the radial distribution of local inflow velocity is taken as the input of conventional BEMT, thus real-time forces on the blade at any circumferential location can be solved. For an *N*-bladed turbine, thrusts and torques on it are assumed to be equal to the summation of forces on all *N* single-blade turbines.

Despite thrust and torque of turbines can be calculated with this approach, serious disadvantages in mathematical precision exist. The inflow is assumed to be uniform with a velocity that equal to the local velocity at the blade element in this approach, so the accuracy of momentum calculation is not sufficient.

Besides, effect of number of blades, *N*, is underestimated as well. The effect of *N* is nonlinear in Eqs.(5) and (6), thus excessive error is introduced when *N*-bladed turbine is simplified to be *N* one-bladed ones. The impact of these disadvantages is to be investigated in this paper to estimate the numerical precise of this approach.

Despite all these numerical disadvantages, the approach is inspiring enough for applying BEMT for solving transient loads on MCTs. As a matter of fact, if transient loads can be solved by BEMT, averaged thrust and power extracted in a rotational period would be solved by integrating transient loads at certain discretized moments. This approach is referred to as Transient-Integration BEMT(TI-BEMT), and mathematical modification of BEMT equations is essential for this approach.

3.2 Modification of momentum consideration

Cylindrical coordinate system (r,θ,z) is introduced, with origin at the center of the blade disk of the turbine, and z axis coincides with the rotation axis. Expansion of slipstream is neglected here, and streamlines are assumed to be straight and parallel to the z axis. According to Bernoulli's equation,

$$\frac{P_1(r,\theta)}{\rho g}+\frac{U_1^2(r,\theta)}{2g}=\frac{P_d^+(r,\theta)}{\rho g}+\frac{U_d^2(r,\theta)}{2g} \tag{7}$$

$$\frac{P_2(r,\theta)}{\rho g}+\frac{U_2^2(r,\theta)}{2g}=\frac{P_d^-(r,\theta)}{\rho g}+\frac{U_d^2(r,\theta)}{2g} \tag{8}$$

where subscript 1 stands for far upstream of the turbine, 2 stands for far downstream, and *d* stands for at the turbine. Superscript "+" stands for near upstream of the turbine, and "-"stands for near downstream. Pressure at far downstream is assumed to equal to that of far upstream, thus

$$P_1(r,\theta)=P_2(r,\theta) \tag{9}$$

Pressure difference between both sides of the turbine disk can be yielded by combining Eqs.(7)~(9):

$$P_d^+(r,\theta)-P_d^-(r,\theta)=\frac{1}{2}\rho\left(U_1^2(r,\theta)-U_2^2(r,\theta)\right) \tag{10}$$

Assuming axial induction factor a is independent from circumferential location, axial velocity at disk and far downstream can be expressed as Eq (11):

$$U_d(r,\theta)=(1-a)U_1(r,\theta) \tag{11}$$

According to actual disk theory, induced velocity at the disk equals to 1/2 of that at far downstream, hence

$$U_2(r,\theta)=(1-2a)U_1(r,\theta) \tag{12}$$

Combine Eqs. (10) and (12):

$$P_d^+(r,\theta)-P_d^-(r,\theta)=\frac{1}{2}\rho U_1^2(r,\theta)4a(1-a) \tag{13}$$

Thrust on an annulus area at radius r, with radial length Δr can be expressed as:

$$\begin{aligned}\Delta T&=\iint\left(P_d^+(r,\theta)-P_d^-(r,\theta)\right)rdrd\theta\\&=\frac{1}{2}\rho 4a(1-a)r\Delta r\int_0^{2\pi}U_1^2(r,\theta)\,d\theta\end{aligned} \tag{14}$$

Define U_T as Eq. (15):

$$U_T^2(r)=\frac{1}{2\pi}\int_0^{2\pi}U_1^2(r,\theta)\,d\theta \tag{15}$$

and thrust can be solved by combining Eqs. (14) and (15):

$$\Delta T=4\pi\rho a(1-a)U_T^2(r)r\Delta r \tag{16}$$

Analogously, torque on that annulus area can be solved by annular momentum difference on both sides of the turbine disk:

$$\begin{aligned}\Delta Q&=\rho\omega_2(r)r^2\iint U_d(r,\theta)rdrd\theta\\&=\rho\omega_2(r)r^3\Delta r\int_0^{2\pi}U_d(r,\theta)\,d\theta\end{aligned} \tag{17}$$

where $\omega_2(r)$ stands for annular velocity at far downstream of the turbine.

Circumferential induction factor *b* is defined as:

$$b=\frac{\omega_d(r)}{\Omega} \tag{18}$$

For inflow without rotation, the annular velocity at the disk and far downstream can be expressed as:

$$\omega_2(r)=2\omega_d(r)=2b\Omega \tag{19}$$

where Ω stands for rotational speed of the turbine. Define U_a as Eq.(20):

$$U_a(r)=\frac{1}{2\pi}\int_0^{2\pi}U_1(r,\theta)\,d\theta \tag{20}$$

and torque can be solved by combining Eqs. (11), (17) and (19):

$$\Delta Q = 4\pi\rho b\Omega U_a(r) r^3 \Delta r(1-a) \tag{21}$$

Thrust and torque are solved by momentum and annular momentum differences. All parameters in Eqs. (16) and (21) are known except induction factors *a* and *b*, which will be solved by combination of blade element consideration.

3.3 Modification of blade element consideration

For an *N*-bladed turbine, *N* blade elements exist at one radial location. Loads on blade elements can be calculated in conventional method. Given the deviation of inflow velocity on each blade element, loads have to be calculated individually, and total loads are solved by summing them up. Lift and drag force of the *i*-th blade element is expressed with reference of (22),(23):

$$\Delta L_i = C_{L,i}\frac{1}{2}\rho U^2(r,\theta_i)c\Delta r \tag{24}$$

$$\Delta D_i = C_{D,i}\frac{1}{2}\rho U^2(r,\theta_i)c\Delta r \tag{25}$$

where $C_{L,i}$ and $C_{D,i}$ stand for lift and drag coefficient of the wing section, c is chord length, and U stands for total velocity at the location of the blade element.

Coefficients are defined as:

$$\begin{aligned} C_{n,i} &= C_{L,i}\cos\varphi_i + C_{D,i}\sin\varphi_i \\ C_{T,i} &= C_{L,i}\sin\varphi_i - C_{D,i}\cos\varphi_i \end{aligned} \tag{26}$$

Geometrical equations can be obtained from the velocity triangle presented in (27)(28):

$$U_1(r,\theta_i)(1-a) = U(r,\theta_i)\sin\varphi_i \tag{29}$$

$$\tan\varphi_i = \frac{U_1(r,\theta_i)(1-a)}{\Omega r(1+b)} \tag{30}$$

Thrust and torque on the *i*-th blade element with radius *r* can be solved by combining Eqs. (22)~(26), and total loads of the *N* blade elements with radius *r* can be expressed as:

$$\Delta T = \frac{1}{2}\rho c\Delta r(1-a)^2 \sum_{i=1}^{N}\frac{C_{n,i}U_1^2(r,\theta_i)}{\sin^2\varphi_i} \tag{31}$$

$$\Delta Q = \frac{1}{2}\rho cr\Delta r(1-a)^2 \sum_{i=1}^{N}\frac{C_{T,i}U_1^2(r,\theta_i)}{\sin^2\varphi_i} \tag{32}$$

3.4 Combination of modified BEMT

Combining Eqs. (16), (21), (27) and (28), the unknown induction factors a and b can be solved:

$$a = \frac{c\sum_{i=1}^{N}\frac{C_{n,i}U_1^2(r,\theta_i)}{\sin^2\varphi_i}}{8\pi rU_T^2(r) + c\sum_{i=1}^{N}\frac{C_{n,i}U_1^2(r,\theta_i)}{\sin^2\varphi_i}} \tag{33}$$

$$b = \frac{c\sum_{i=1}^{N}\frac{C_{T,i}U_1^2(r,\theta_i)}{\sin 2\varphi_i}}{4\pi rU_a - c\sum_{i=1}^{N}\frac{C_{T,i}U_1^2(r,\theta_i)}{\sin 2\varphi_i}} \tag{34}$$

Eqs. (29) and (30) have to be solved by iteration due to the mutual effect between induction factors and φ_i. Thrust and torque at the radius *r* would be solved then by Eqs. (16) and (21), as the induction factors are known. Loads on the turbine can be solved by numerical integration. Correction for hub/tip loss and turbulence component is provided by He, YP. (2013) in conventional BEMT, which is applicable for the modified approach.

3.5 Time-averaged approach

TI-BEMT, as is discussed previously, requires integration of transient loads in a rotation period, which will cost much computation efforts. One simple treatment is applying averaged inflow velocity in a rotational period in blade element consideration, while momentum is considered the same way as TI-BEMT. This approach is referred as Time-Averaged BEMT(TA-BEMT). In this approach, averaged local inflow velocity of a blade element in a rotation period is solved and taken as the input in blade element consideration. Therefore, the inflow velocity applied is time-independent and the integration is not required.

For turbines which rotate with a constant speed and work in steady inflow, the time-averaged inflow velocity of a blade element at the radius *r* equals to the averaged velocity in the annulus area at radius *r*, with radial length Δr, which can be solved by Eqs. (20). Momentum changes are considered by Eqs. (16) and (21). Equations to solve induction factors are yielded by combination of both considerations, as:

$$a(r) = \frac{cNC_nU_a^2(r)}{8\pi rU_T^2(r)\sin^2\varphi + cNC_nU_a^2(r)} \tag{35}$$

$$b(r) = \frac{cNC_T}{8\pi r\sin\varphi\cos\varphi - cNC_T} \tag{36}$$

This approach avoided discretization of rotation period, and loads on each blade element does not have to be calculated individually, hence efficiency of simulation is improved. However, the real-time variation of local inflow speed is neglected here, which could be a major disadvantage for the accuracy of TA approach.

4. CASE STUDY

4.1 Geometry particulars of turbine

Experiment on a model turbine is conducted by Bahaj, A.S. et al.(2007), and the turbine is applied for numerical analysis in this paper. The turbine is three-bladed, whose diameter is D=0.8m. The blades are developed from hydrofoil of NACA-638xx, and distributions of chord length, twist angle and thickness of blades are given by Table 1.

Table 1 Particulars of turbine blades (Bahaj, A.S. et al.(2007))

r(mm)	c/R	Twist angle(deg)	t/c(%)
80	0.125	20.0	24.0
120	0.116	14.5	20.7
160	0.106	11.1	18.7
200	0.097	8.9	17.6
240	0.088	7.4	16.6
280	0.078	6.5	15.6
320	0.069	5.9	14.6
360	0.059	5.4	13.6
400	0.050	5.0	12.6

Numerical analysis is conducted with both CFD and BEMT. In this paper, CFD analysis for this turbine is conducted based on the RANS solver, which has been developed by Li, H. et al.(2016). The flow field consists of rotating domain and stationary domain, as is shown in Figure 3. Rotation domain is shaped as a cylinder that rotates at the speed of the turbine, with a diameter of 0.82m and a length of 0.4m, while the MCT is located at center of it. Stationary domain is shaped as a cuboid whose length is 10D while both width and height equal to 4D.

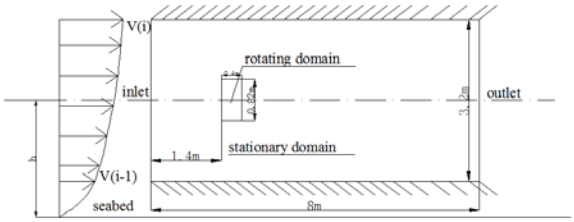

Figure 3 Sketch of the computational domain in uniform inflow(Li,H. et al.(2016))

The computational domains are discretized by structural mesh produced by ANSYS ICEM CFD. Grids of computational domains is presented in Figure 4, and mesh of the rotating domain is presented in Figure 5, while numbers of elements in this simulation are given by Table 2, and Y+ in this analysis are within 50.

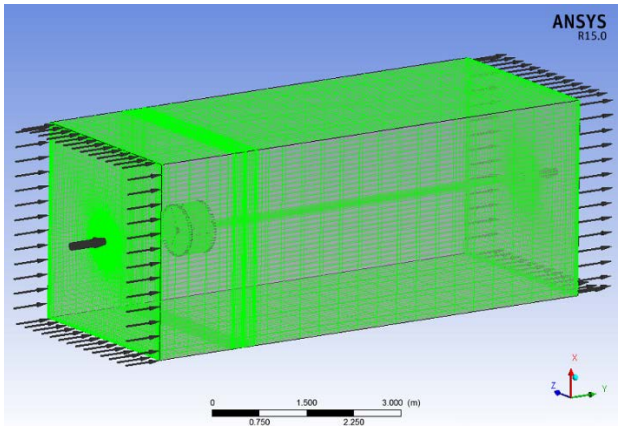

Figure 4 Mesh of computational domains

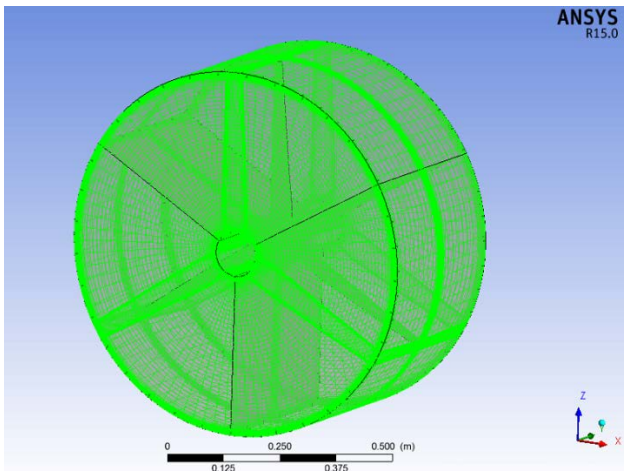

Figure 5 Mesh of rotating domain

Table 2 Numbers of elements in computational domains

Domain	Number of elements
Stationary domain	1,314,400
Rotating domain	1,103,250
Summary	2,417,650

4.2 Analysis of a MCT in uniform inflow

At first, the turbine is placed in uniform inflow with velocity of 1.73m/s inflow speed and rotates with the speed of 17.3rad/s. Nondimensional coefficients, i.e. power coefficient(C_P) and thrust coefficient(C_T) are defined as Eqs. (33) and (34) to estimate performance of turbines, and their values are given in Table 3.

$$C_P = \frac{Q\omega}{\frac{1}{2}\rho V_0^3 \pi R^2} \tag{37}$$

$$C_T = \frac{T}{\frac{1}{2}\rho V_0^2 \pi R^2} \tag{38}$$

Table 3 Comparison of simulation of CFD and BEMT

Simulation method	C_P	Error	C_T	Error
Experiment (Bahaj, A.S. et al.(2007))	0.3752	-	0.6302	-
CFD	0.3615	-3.66%	0.5225	-17.10%
Conventional BEMT	0.3615	-3.66%	0.5400	-14.32%

According to Table 3, hydrodynamic coefficients calculated by both numerical methods are lower than experiment results. For CFD analysis, the error is 3.66% for C_P and 17.10% for C_T, while for BEMT, the error is 3.66% for C_P and 14.32% for C_T. However, results of both numerical methods agree with each other.

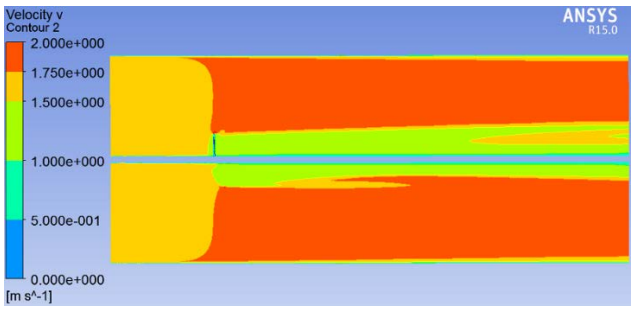

Figure 6 Contour and vector of axial velocity distribution in uniform inflow

Contour of axial velocity distribution is given in Figure 6, according to which that the inflow velocity at upstream of turbine is 1.73m/s, while velocity downstream is within 1~1.5m/s, hence a significant velocity decrease exists in the slipstream of turbine, which demonstrates that kinetic energy of marine current is extracted by the turbine. Due to the expansion of the slipstream, the region out of the slipstream at downstream of the turbine has larger velocity than 1.75m/s.

To demonstrate the pressure distribution on blades, pressure coefficient C_{press} is defined as Eq. (35)

$$C_{press} = \frac{p}{\frac{1}{2}\rho V_0^2} \tag{39}$$

where ρ stands for density of fluid, and V_0 stands for flow velocity at far upstream of turbine. Contours of C_{press} distribution on both pressure side and suction side of a blade are given in Figure 7. There is a large area of negative pressure on the suction side, where cavitation is likely to occur, while high pressure exist at leading edge and tip of trailing edge on pressure side. Apparently, pressure difference exists between both sides of the blade, which generates the thrust and torque acting on the blade. Therefore, despite hydrodynamic coefficients of CFD analysis has certain difference with experiment data, the flow field feature obtained from this simulation is reasonable.

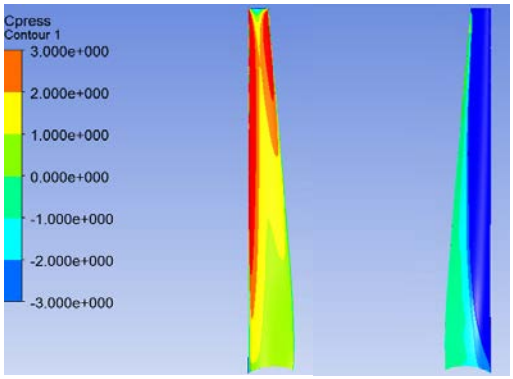

a) Pressure side b) Suction side

Figure 7 Contour of pressure coefficient distribution on a blade

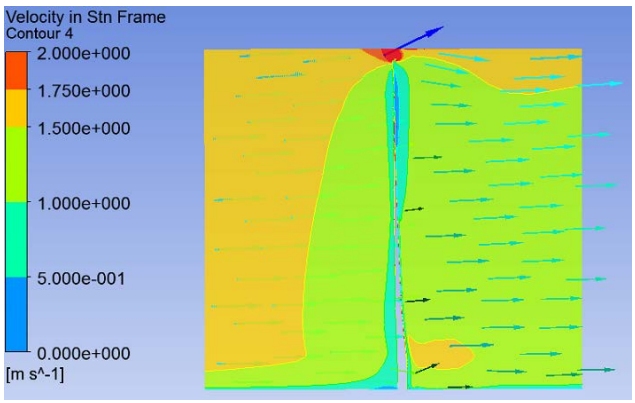

Figure 8 Vector of velocity in rational domain (in uniform flow)

Velocity vector in rotational domain is presented in Figure 8. It can be observed that radial velocity component is more significant at tip of the blade, and expansion exists at near downstream of the blade, which demonstrates that the flow field is disturbed by the turbine.

4.3 CFD Analysis with different submergence of MCT

In research on MCTs, the inflow is ordinary assumed to be uniform; while for actual sea flow, due to the existence of friction of seabed, inflow velocity varies with water depth. For coastal water, velocity profile is estimated assumingly to be a power law for preliminary prediction. In this paper, distribution of axial velocity is estimated as Eq.(36):

$$v(z) = V_0\left(\frac{z+h}{H}\right)^{\frac{1}{7}} \tag{40}$$

where H is depth of the water, and V_0 is the mean velocity of inflow, and h is the vertical distance between the seabed and rotation axis of the turbine, hence a turbine with higher h has a shallower immersion. In this paper, V_0 =1.73m/s, H =3.2m, and h varies from 0.8~3.2m, with a step of 0.8m.

Due to the lack of experimental results in non-uniform inflow, CFD is applied for prediction of MCTs. The analysis is based on the numerical model in uniform inflow as well, except inflow condition differs. Both steady state and transient computation are carried out. Apparently, transient analysis is more accurate option for simulation of a flow field with changing boundary condition, yet it consumes much more time than steady analysis as well. For MCTs that work in uniform inflow, although changing boundaries exist when MCTs are rotating, steady analysis is a common option because transient behavior is not so prominent.

Table 4 gives the results of the simulations, and results in uniform flow are given as well to demonstrate the impact of velocity profile on MCT performance.

Table 4 Comparison of MCT performance in uniform flow and shear flow

h	C_P		C_T	
	Shear	Difference (Uniform= 0.3615)	Shear	Difference (Uniform=0. 5225)
0.8	0.2277	-38.84%	0.4129	-22.18%
1.6	0.2945	-20.74%	0.4709	-11.09%
2.4	0.3380	-8.93%	0.5046	-4.59%
3.2	0.3702	-0.07%	0.5278	-0.04%

According to Table 4, C_P and C_T in shear flow are close to those in uniform flow when h=3.2m, because the inflow velocity equals to the speed of uniform inflow. For cases with deeper submergence, C_P and C_T in shear flow are smaller than in uniform inflow, due to the decrease of inflow velocity.

Besides, according to Table 4, both C_P and C_T decrease when submergence increases, while percentage of power loss is larger than thrust with same submergence, therefore shallow submergence is more recommendable for energy extraction of MCTs, while deep submergence is more recommendable for reducing loads on positioning system.

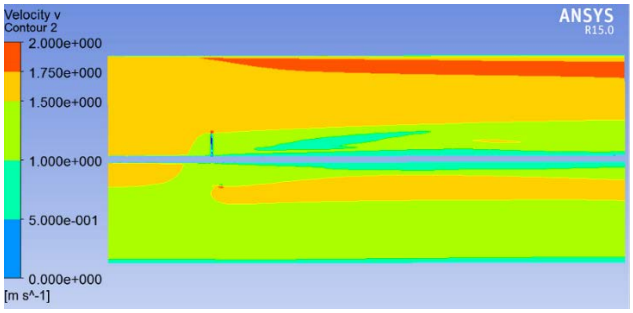

Figure 9 Contour of axial velocity distribution in shear flow (h=1.6m, steady state)

Contour of axial velocity distribution when h=1.6m is given by Figure 9, according to which the velocity has certain asymmetry due to the velocity profile. Velocity at both upstream and downstream are smaller compared with uniform inflow, while a decrease exists in slipstream as well. Velocity vector is also given in Figure 9, and in terms of composition of velocity vector, circumferential component prevails in rotational domain, and axial component prevails in stationary domain, which agrees with the feature in uniform inflow.

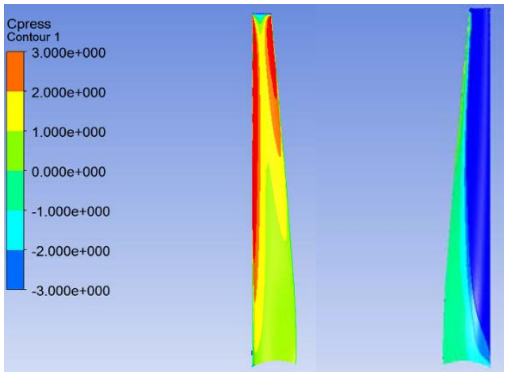

a) Pressure side b) Suction side

Figure 10 Contour of pressure coefficient in shear flow(h=1.6m, steady state)

Pressure distribution is given by Figure 10. Compared with the contour with uniform inflow, the pressure distribution is similar while the high pressure area on pressure side is smaller, which demonstrates that the pressure difference between both sides of this blade are smaller than on the blade in uniform inflow, hence thrust and torque are smaller.

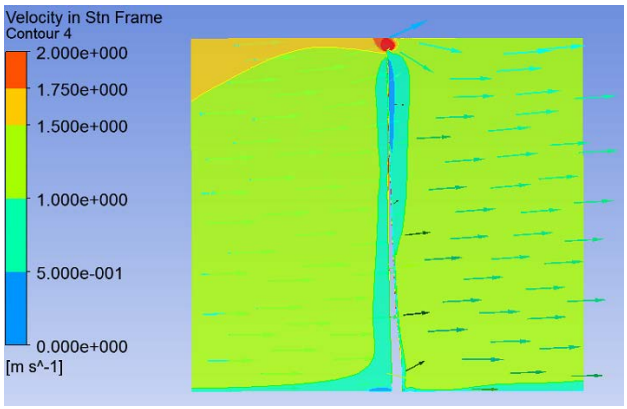

Figure 11 Vector of velocity in rotational domain (h=1.6m, steady state)

Velocity vector in rotational domain is presented by Figure 11. Compared with Figure 8, a similar disturbance exists in this figure. However, the area where the flow field is disturbed near the tip is smaller than in Figure 8, while radial velocity component is less significant as well. It is demonstrated that the flow field is less disturbed by the blade in shear flow.

4.4 Comparative Study of Transient Behavior on MCT

Since the inflow has certain level of non-uniformity, effect of transient behavior on a MCT performance is worth discussion. Transient analysis is carried out based on the same computational model, and the outputs are given by Table 5. Both power and thrust coefficients of transient analysis is larger than steady state analysis, by 2~3% for C_P and 1~2% for C_T, which is caused by transient behavior of flow field.

Table 5 Comparison of CFD analysis with transient and steady option

h	C_P			C_T		
	Transient	Steady	Error/%	Transient	Steady	Error/%
3.2	0.370	0.361	-2.42	0.5278	0.5223	-1.05

5. RESULTS AND DISCUSSION

5.1 Comparative Study between previous approach and TI-BEMT

Previous approach for transient force has several mathematical disadvantages, their impact can be quantified

by applying this approach for performance prediction for the turbine in uniform inflow, and compare the results to that of conventional BEMT, which is given by Table 6. Torque prediction has error of 10% and thrust error is up to 24%. That demonstrates that previous approach doesn't agree with conventional theory in the same inflow condition.

Results of TI-BEMT approaches in the same inflow condition are given by Table 6 as well, according to which the results highly agree with the conventional theory. Therefore, TI-BEMT is of better accuracy than previous approach for calculation of transient force acting on a turbine.

Table 6 Comparison of approaches

Approaches	C_P	Error/ %	C_T	Error/ %
Conventional BEMT	0.3615	-	0.5400	-
Previous approach	0.3237	-10.46	0.4101	-24.06
TI-BEMT	0.3615	0.00	0.5400	0.00

5.2 Comparative Study between M-BEMT and CFD

Hydrodynamic coefficients of MCTs are calculated by both modified BEMT approaches, and compared with that of steady CFD to evaluate their accuracy. The comparison is given by Figure 12, and error of C_P and C_T are defined as Eq. (37).

$$Error\left(C_{P(T)}\right)=\frac{C_{P(T),\mathrm{BEMT}}-C_{P(T),CFD}}{C_{P(T),CFD}}\times 100\% \qquad (41)$$

Powers and thrusts predicted by modified BEMT are both larger than results of CFD in the same inflow condition. C_P results predicted by both modified BEMT approaches highly agree with each other, and are larger than that of CFD analysis by a maximum error of 5%. When h=3.2m, i.e. in shallow submergence, results of both modified BEMT approaches are highly close to CFD. For C_T, results of TA-BEMT approach are larger than TI-BEMT approach, and they both have better accuracy for shallow-submergence cases. For turbines with deep submergence, the error is within 10% for TA-BEMT approach and 6% for TI-BEMT. Therefore, both M-BEMT approaches have reasonable outputs, especially for turbines with shallow submergence, and TI-BEMT is the more proper than the other.

Compared with C_P of transient CFD, outputs of modified BEMT become smaller than transient CFD when h>1.6m, while still larger for cases with deeper submergence, with the maximum error of 2.5%. For C_T, results of M-BEMT are larger but closer to that of transient CFD, while the maximum error is approximately 8% for TA approach and 4% for TI approach. Therefore, accuracy of M-BEMT is better when compared with CFD analysis since transient behavior is taken into account.

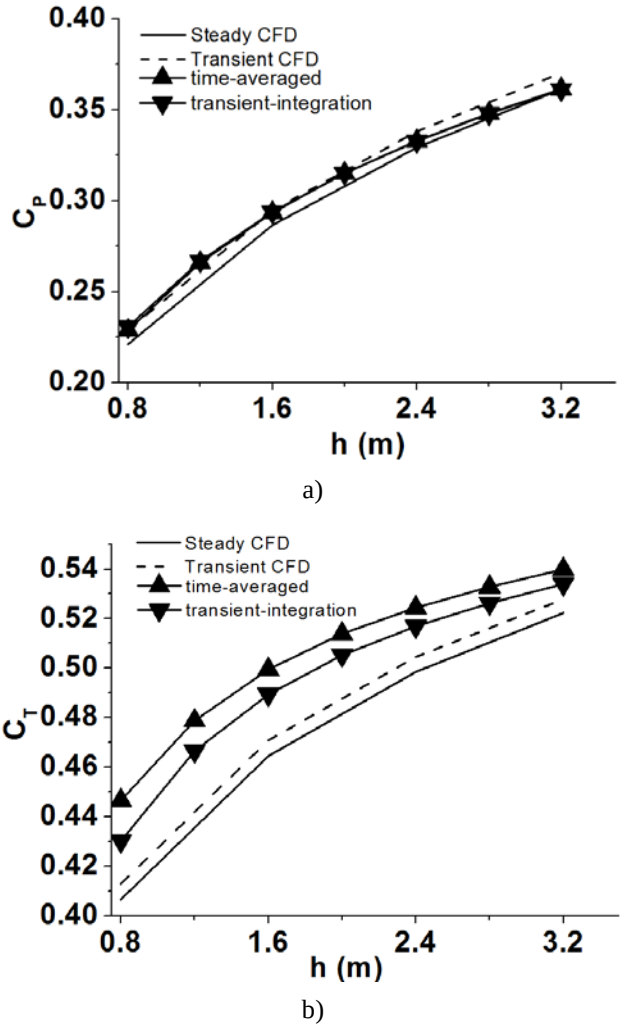

Figure 12 Comparison of power and thrust coefficients solved by BEMT and CFD a) Power coefficients b)Thrust coefficients

In comparison between the M-BEMT approaches, TA approach has a slightly better accuracy for C_P, yet much less accurate for C_T, the reason of which is that the inflow speed input of TA-BEMT is too simplified to achieve the accuracy of TI-BEMT approach. Although the computation of TI approach is more significant than TA-BEMT, it is worthy because one simulation takes only a few minutes, which is still acceptable for most cases. In conclusion, TI-BEMT is the more recommendable approach for performance analysis MCTs in non-uniform inflow.

6. CONCLUSION

In this paper, two modified BEMT approaches, Time-Averaged(TA-BEMT) and Transient Integration(TI-BEMT), are developed, and are applied for performance analysis for MCTs in shear flow. CFD analysis is carried out to validate their accuracy, with options of steady state

and transient, so that impact of transient behavior on the flow field is quantified. Besides, impact of submergence on hydrodynamic performance of a MCT in shear flow is investigated with numerical models developed in this paper.

According to this research, turbines in shear flow have smaller thrust and power than uniform flow due to the velocity profile, and turbines with shallow submergence are more efficient for energy extraction, while deep submergence is helpful for reducing loads of positioning system of turbines.

According to CFD analysis, power and thrust coefficients calculated by transient analysis is larger than that of steady analysis, by 2~3% for C_P and 1~2% for C_T. Accuracy of M-BEMT approaches is estimated by comparison with CFD. Power coefficient prediction of both M-BEMT approaches are close, with errors within 2.5% compared with CFD; while TI-BEMT approach is of better accuracy than TA-BEMT, with a maximum error of 4.2%. It demonstrates both approaches have reasonable accuracy, and TI-BEMT is the relatively more accurate and more recommendable between them. Given the advantage of high efficiency, numerical models developed in this paper are functional and effective tools for MCT performance prediction.

ACKNOWLEDGEMENTS

This research was supported by the State Key Laboratory of Ocean Engineering (GKZD010063) and the National Basic Research Program of China ("973" Program) with Grant No. 2014CB046200.

REFERENCE

Bahaj, A.S., Batten, W.M.J., McCann, G. (2007). 'Experimental verification of numerical predictions for the hydrodynamic performance of horizontal axis marine current turbines'. Renewable energy, 32, 2479-2490.

Batten, W.M.J., Bahaj, A.S., et al. (2008). The prediction of the hydrodynamic performance of marine current turbines. Renewable energy, 33, 1085-1096.

He, YP. (2013). 'Designing and research on the blades and floating support structure of a horizontal-axis current turbine'. Master thesis, Shanghai Jiao Tong University, China.

Klein, L., Schulz, C., et al. (2016). 'Influence of jet flow on the aerodynamics of a floating model of wind turbine'. Proc 26th International Ocean and Polar Engineering Conference, Rhodes Island, Greece, 26 June-2 July.

Li, H., Yu, L., et al. (2016). 'Numerical Comparative Study for Marine Current Turbine in Steady Uniform and Shear Inflow'. Proc 12th ISOPE PACOMS Symposium, Gold Coast/Brisbane, Australia, 3-7 October.

Wang, Y., Yu, L., Du, WK., et al. (2014). 'Development of An Optimization Approach from hydrofoil to Blade for A Horizontal Axis Marine Current Turbine'. Proc 1st International Conference on Renewable Energies Offshore, IST – Lisbon, Portugal.

Yu, L., Li, H., et al. (2016). 'Development of An Optimal Approach from Hydrofoil to Blade for A Horizontal Axis Marine Current Turbine'. Proc 26th International Ocean and Polar Engineering Conference, Greece, 26 June-2 July.

DISCUSSION

Question from Shin Hyung Rhee

1, How did you obtain C_L,C_D for your blade sections.
2, Did you check the resolution sensitivity of spanwise direction spacing, now that you have varying inflow onto each blade section?

Author's closure

1, Xfoil is used for calculating C_L,C_D.

2, Yes, we have checked different division both spanwise and circumferential, it converged in a reasonable fine number of sections. For this case the thrust force decreases maximum 2.5% when the spanwise division has been set to be 9, 17, 33 and 66. The third number has been chosen for the computation. The circumferential division is also important for this case it has been settled around 60.

Question from Chen-Jun Yang

In the current turbine case is it necessary to consider the sea bottom effects on turbine performance, and how to do it with your methods?

Author's closure

The current turbine is a shallow immerged type in order to obtain high energy extraction effect due to the shear inflow, so that the bottom effects is not considered in this model. For sure, the bottom effect will cause the flow velocity significantly decreased, we think not only the velocity loss but additional friction drag have to be considered.

Question from José Falcão de Campos

If the turbine is operating in shear flow, the flow is unsteady in the reference frame attached to the blades. How do you take into account the unsteady effects on the lift acting on the blade sections in the transient integration model?

Author's closure

The transient model is dependent to the unsteady inflow. At specified postion of the blade on the disk, the local velocity is applied to the transient integration model at each section to include unsteady effect with both axial and circumferential velocities, then the lift and drag forces are calculated by Xfoil. Consequently, the blade performance can be integrated with all the sections.